Solar Phys (2008) 249: 369–380
DOI 10.1007/s11207-008-9185-9

Gnevyshev Peaks and Gaps for Coronal Mass Ejections of Different Widths Originating in Different Solar Position Angles

R.P. Kane

Received: 21 October 2007 / Accepted: 2 April 2008 / Published online: 15 May 2008

Abstract The sunspot number series at the peak of sunspot activity often has two or three peaks (Gnevyshev peaks; Gnevyshev, *Solar Phys.* **1**, 107, 1967; *Solar Phys.* **51**, 175, 1977). The sunspot group number (SGN) data were examined for 1997 – 2003 (part of cycle 23) and compared with data for coronal mass ejection (CME) events. It was noticed that they exhibited mostly two Gnevyshev peaks in each of the four latitude belts 0° – 10°, 10° – 20°, 20 ° – 30°, and > 30°, in both N (northern) and S (southern) solar hemispheres. The SGN were confined to within latitudes ± 50° around the Equator, mostly around ± 35°, and seemed to occur later in lower latitudes, indicating possible latitudinal migration as in the Maunder butterfly diagrams. In CMEs, less energetic CMEs (of widths < 71°) showed prominent Gnevyshev peaks during sunspot maximum years in almost all latitude belts, including near the poles. The CME activity lasted longer than the SGN activity. However, the CME peaks did not match the SGN peaks and were almost simultaneous at different latitudes, indicating no latitudinal migration. In energetic CMEs including halo CMEs, the Gnevyshev peaks were obscure and ill-defined. The solar polar magnetic fields show polarity reversal during sunspot maximum years, first at the North Pole and, a few months later, at the South Pole. However, the CME peaks and gaps did not match with the magnetic field reversal times, preceding them by several months, rendering any cause – effect relationship doubtful.

1. Introduction

The sunspot number series at the peak of sunspot activity often has two or three peaks. Gnevyshev (1967) concluded that the 11-year cycle does not contain one but two waves of activity with different physical properties. In cycle 19 (1954 – 1964), the coronal line half-yearly average intensity at the 5303 Å green line actually had two maxima, the first one in 1957 and the second in 1959 – 1960. During the first maximum of 1957, the intensity increased and subsequently decreased simultaneously at all latitudes. The second maximum of 1959 – 1960 occurred only at low latitudes, i.e. for latitudes < 15°; this maximum was bigger

R.P. Kane (✉)
Instituto Nacional de Pesquisas Espaciais – INPE, C.P. 515, 12245-970 São José dos Campos, SP, Brazil
e-mail: kane@dge.inpe.br

than the first one, and the pattern was seen in both hemispheres (Antalova and Gnevyshev, 1965). The plots for latitudes 15° – 20° showed both of the maxima, indicating that the second maximum visible for latitudes 0° – 10° is a separate phenomenon and not the result of a shift of the first maximum from high latitudes in the first part of the sunspot cycle to low latitudes near the end of the cycle. In a later paper, Gnevyshev (1977) examined coronal data for cycle 20 (1965 – 1974) also and reported that, for several solar and geophysical parameters, the first maximum was almost simultaneous. It was seen for solar activity at all heliographic latitudes but was maximal near latitude 25° in each hemisphere. Antalova and Gnevyshev (1983) recognized the existence of more peaks, often a third peak during a cycle. Feminella and Storini (1997) examined the long-term behavior of several solar activity parameters (spots, flares, radio, and X-ray fluxes), confirmed the double peaks, and found that the peaks are more distinct with a clear gap in between, when intense and/or long-lasting events are considered. Low-energy and short-duration events tend to follow a single-peaked 11-year cycle. The double peaks are reported to be detected in all the solar atmospheric layers – photosphere, chromosphere, and corona – out to interplanetary space. Double peaks have also been detected in cosmic-ray modulation (*e.g.*, Storini and Pase, 1995). In Kane (2002, 2003), the evolution of various solar indices around sunspot maximum (two peaks in 12-month running means) is shown to occur almost simultaneously within a month or two and the gap between the two peaks is shown to be clearer for higher energy indices such as X-ray flux. Whereas the peaks are seen more distinctly in solar indices at narrow latitude belts, solar parameters characterizing full-disk activity do not reveal the peaks distinctly, though distinction is better for intense events (big sunspots, big flares, etc.) and for indices originating higher up in the solar atmosphere (Feminella and Storini, 1997). The double peaks have not been given any name as such. We have termed these as "Gnevyshev peaks," but the gap in between has been termed by Storini and Pase (1995) as the "Gnevyshev gap" (GG).

As an explanation for the presence of a GG, Obridko and Shelting (1992) suggested a link between outstanding activity phenomena and the strength of the *heliomagnetic field*. On this basis, during the inversion of the polar heliomagnetic field, a decrease or a gap GG in the number of high-energy events occurs (for details see Storini *et al.*, 2003). Feminella and Storini (1997) and, later, Alania *et al.* (1999) suggested that in the course of Sun's polar magnetic field reversal, a part of the Sun's energy is used up for this reversal process. All this is claimed to be intimately related to the *solar polar magnetic field reversals*, first at the North Pole and a few months later at the South Pole, which occur about every 11 years when sunspot activity is at the maximum. Every alternate cycle, the polarity sign reverses, thus indicating a 22-year Hale magnetic cycle. This has implications for cosmic-ray (CR) modulation, which shows broader hysteresis loops between CR modulation and sunspot number in odd cycles 19, 21, and the recently ended cycle 23, as compared to even cycles 20 and 22. Jokipii and Thomas (1981) explained this difference as due to drift mechanisms, which give opposite effects with the changing sign of the solar polar magnetic field. This also implies that the CR flux should show gaps exactly similar to the sunspot GG gaps, and both should start simultaneously with the solar magnetic pole reversal. However, Kane (2006a) pointed out that the beginnings of CR gaps and the sunspot GG gaps were not simultaneous, and both occurred *several months earlier* than the beginning of the North Pole magnetic field reversal, indicating that the field reversals could not be a direct cause of CR gaps, as effect cannot precede the cause.

An important solar parameter, namely, coronal mass ejections (CMEs) (Tousey, 1973; Munro *et al.*, 1979; Webb and Howard, 1994; Cliver and Hudson, 2002), examined by Kane (2006a, 2006b, 2008) for cycle 23, showed a variation near sunspot maximum somewhat different from that of sunspots and other activity. The CME data used in Kane (2008) were

for all CMEs, but there was a preliminary indication that the variations of CMEs of different energies could be different. In the present communication, the Gnevyshev peaks and gaps for CMEs of different widths originating at different position angles are examined and compared with sunspot activity for years 1997 – 2003 near the maximum of cycle 23.

2. Data

Data for sunspot numbers at different solar latitudes were not available to us. However, David Hathaway of NASA has scrutinized and used all the earlier and recent data of *sunspot groups*, normalized them to produce a reliable continuous data series from 1874 up to date, and presented these on the Web at http://solarscience.msfc.nasa.gov/greenwch.shtml. From these, we counted the *number* of sunspot groups and obtained SGNs (sunspot group numbers) for successive three-month periods (January, February, and March (JFM); April, May, and June (AMJ); July, August, and September (JAS); and October, November, and December (OND)). It was shown in Kane (2008) that SGN was a good proxy for the conventional sunspot number *Rz*, when whole-disk values were compared. Information about CMEs was obtained from the NASA GSFC CDAW Data Center Web site http://cdaw.gsfc.nasa.gov/CME_list/index.html, which has the LASCO CME Catalog. The CME data are given for position angles (PA) around the solar disk, from North Pole (0°) to South Pole (180°) on the eastern side and then back from South Pole (180°) to North Pole (360°) on the western side of the solar disk. Thus, for each latitude band, there are two sets of position angles, one for the eastern side and another for the western side. Here, the two values within the same N and SPA bands on the eastern and western sides were summed together as follows: 0° – 5° was added to 360° – 355°, 5° – 10° was added to 355° – 350°, and so on until, finally, 175° – 180° was added to 180° – 185°. Data used are for the interval 1997 – 2003, which showed the Gnevyshev peaks and gaps prominently. By assuming arbitrarily that larger widths most probably imply larger energies, the CME data are divided into four groups: very weak (of width 0° – 35°), weak (of width 36° – 70°), strong (of width 71° – 105°), and very strong (of width > 105°). Further, the numbers of CMEs are counted separately for the position angle belts 0° – 10°, 10° – 20°, 20° – 30°, 30° – 40°, 40° – 60°, and 60° – 90° in N (northern) and S (southern) hemispheres of the Sun, for each three-month interval JFM, AMJ, JAS, and OND. These belts are chosen to give sufficient numbers in each but to have at least three or four belts to compare with SGNs, which are mostly concentrated within ± 35° of the solar equator. Further, running means are obtained for four consecutive three-month means, thus yielding 12-month running means, centered three months apart (four values per year).

3. Plots of SGN and Very Weak CMEs (of Width 0 – 35°) for 1997 – 2003

Figure 1 shows the plots of 12-month running means (four values per year) for 1997 – 2003. The top plots (a) are for sunspot group numbers for latitude belts 0° – 10° N, 10° – 20° N, 20° – 30° N, and >30° N. The maxima are indicated by big dots, and simultaneous maxima at successive latitudes are joined by lines. As can be seen, every belt shows at least two SGN maxima (Gnevyshev peaks), which seem to occur later at lower latitudes, suggesting latitudinal migration as in the Maunder butterfly diagrams (Spörer sunspot law). This pattern is different from that of cycles 19 and 20 described in Gnevyshev (1967, 1977). Figure 1(b) shows similar plots for the *very weak* CMEs (of width 0 – 35°). The following may be noted in Figure 1(b):

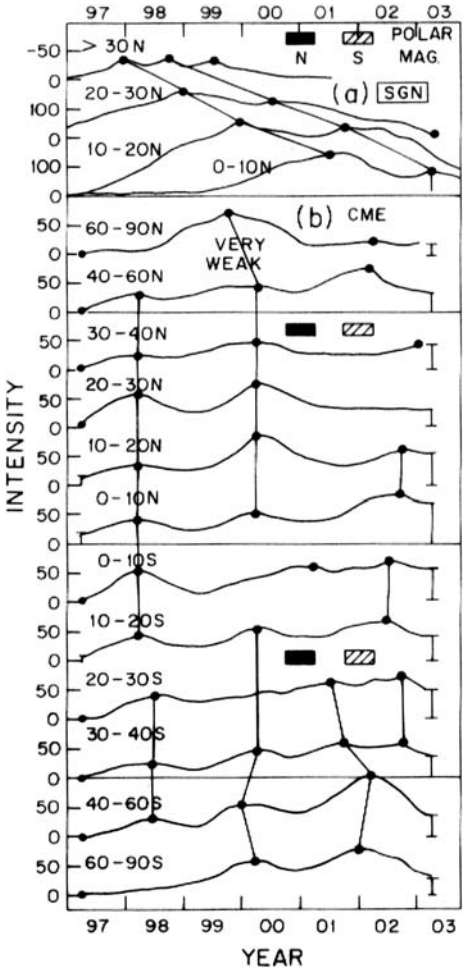

Figure 1 Plots of intensity and number of events of 12-month running means (four values per year) for 1997 – 2003. (a) Sunspot group numbers SGN, for latitude belts 0° – 10° N, 10° – 20° N, 20° – 30° N, and > 30° N. The maxima are indicated by big dots. Almost simultaneous maxima at successive latitudes are joined by lines. (b) Similar plots for the very weak CMEs (of width 0° – 35°). The rectangles mark the solar polar magnetic field reversals, with a solid rectangle for the North Pole and a hatched rectangle for the South Pole.

(1) All the plots show two or more peaks (mostly three) that match among themselves (*i.e.*, are joined by almost vertical lines) but none of which match with the SGN peaks completely. The Gnevyshev peaks of SGN and CMEs are essentially dissimilar, in both locations and lengths of Gnevyshev gaps, with 18 – 21 months for SGN and ∼ 24 months or more for CMEs. However, there is a slight indication that the first CME peak in early 1998 may have an approximate resemblance to the first peak of SGN at high latitudes (> 30° N).

(2) In the top and also at places further down, the full rectangle indicates the reversal of the magnetic field at the solar North Pole, reported to have occurred variously as during October 2000 (Harvey and Recely, 2002), or February 2001 (Bilenko, 2002), or May 2001 (Durant and Wilson, 2003). The hatched rectangle indicates the reversal of the magnetic field at the solar South Pole, during October 2001 (Harvey and Recely, 2002), or September 2001 (Durant and Wilson, 2003), or January 2002 (Bilenko, 2002). The Gnevyshev peaks of CMEs do not match the beginnings of the magnetic reversals even roughly and occur often much earlier. Thus, any cause-and-effect relationship between the CME peaks and gaps with magnetic field reversals seems dubious.

Table 1 Number of CMEs of different widths and their percentages in different (30°) latitude belts.

Latitude	Number of CMEs					%
	Very weak	Weak	Strong	Very strong	Total	
60° – 90° N	74	85	30	21	210	10
30° – 60° N	110	126	44	37	317	15
0° – 30° N	215	158	76	73	522	25
0° – 30° S	209	160	66	71	506	24
30° – 60° S	159	119	49	40	367	17
60° – 90° S	76	64	30	24	194	9
Total	843	712	295	266	2116	100

(3) In contrast to SGNs, which are confined mostly to latitudes between 35° N and 35° S, the number of CMEs is spread in all latitudes, though not uniformly. The numbers for 30° latitude belts are given in Table 1. There is a higher concentration in low latitudes, which drops to about half at middle latitudes, and about one-third at polar latitudes. Gopalswamy *et al.* (2003) separated high-latitude (HL) and low-latitude (LL) CMEs, designated the LL as related to sunspots and the HL as related to PCFs (polar crown filaments), and mentioned that some HL cessations were related to the solar polar magnetic field reversals. In Figure 1, neither CMEs at 60° – 90° N (one major peak) nor those at 60° – 90° S (two peaks and a trough in between) match exactly with the magnetic field reversals (full and hatched rectangles).

4. Plots of SGN and Weak CMEs (of Width 36° – 70°) for 1997 – 2003

Figure 2 shows similar plots for weak CMEs (of width 36° – 70°). The top plots (a) are for SGN as in Figure 1(a). The other plots (b) are for weak CMEs. The following may be noted:

(1) All CME plots have two or more peaks (mostly three), none matching with the SGN peaks, which show latitudinal migration. Peaks in successive latitudes are not always simultaneous (*i.e.*, the joining lines are not always completely vertical), but systematic latitudinal migration is not indicated for CME peaks.
(2) No relationship with solar polar magnetic field reversals (full and hatched rectangles) is indicated.
(3) The numbers for 30° latitude belts are given in Table 1. There is a higher concentration in low latitudes, which drops to about three-fourths at middle latitudes, and to about half at polar latitudes. Thus, weak events have spread more to middle and higher latitudes, as compared to very weak events.
(4) Similar to what is seen in Figure 1, the value at the last point (in 2003) in all CME plots is far above the 1997 level. However, in contrast to Figure 1 where the initial value in 1997 was low, the CME value of 0° – 10° N in Figure 2 is very high, indicating that extra CME activity can occur in some low latitudes even at the beginning of sunspot activity.

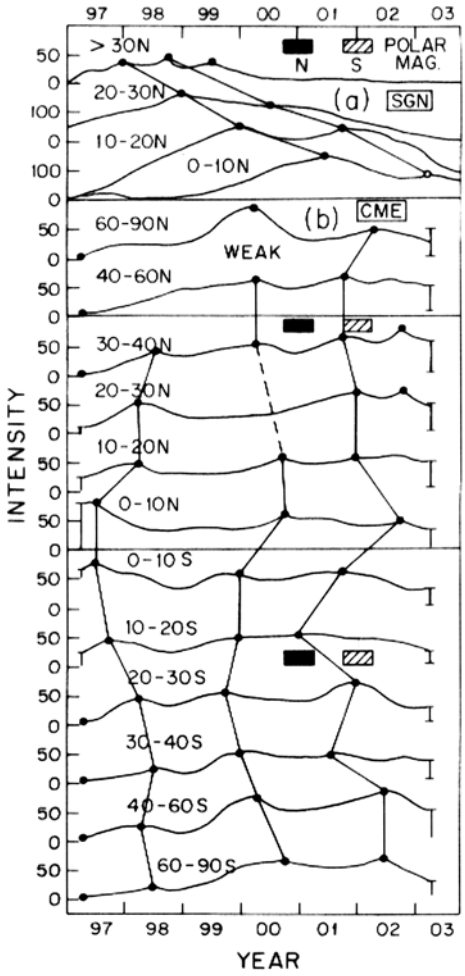

Figure 2 Same as Figure 1, but for weak CMEs (of width 36° – 70°)

5. Plots of SGN and Strong CMEs (of Width 71° – 105°) for 1997 – 2003

Figure 3 shows similar plots for strong CMEs (of width 71° – 105°). The top plots (a) are for SGN, as in Figure 1(a). The other plots (b) are for strong CMEs. The following may be noted:

(1) All CME plots have two or more peaks (mostly three), none matching with the SGN peaks, which showed latitudinal migration. Peaks in successive latitudes are not always simultaneous (*i.e.*, the joining lines are not always completely vertical), but systematic latitudinal migration is not indicated.
(2) No relationship with solar polar magnetic field reversals (full and hatched rectangles) is indicated.
(3) The numbers for 30° latitude belts are given in Table 1. There is a higher concentration in low latitudes, which drops to two-thirds at middle latitudes, and to less than half at polar latitudes.
(4) In contrast to Figure 1 where the initial value in 1997 was low, the CME values for 10° – 20° N, 0° – 10° N, and 0° – 10° S in Figure 3 (vertical bars) are very high, indicating that

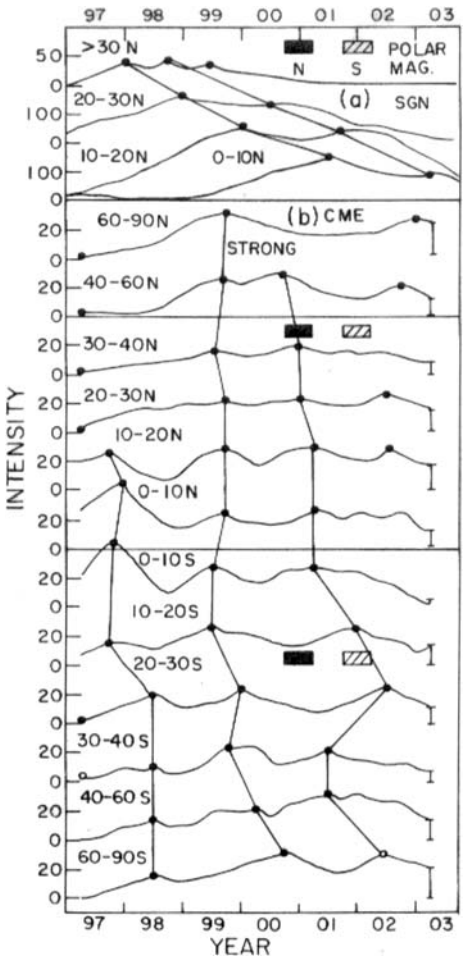

Figure 3 Same as Figure 1, but for strong CMEs (of width 71° –105°)

extra CME activity can occur in some low latitudes even at the beginning of sunspot activity.

6. Plots of SGN and Very Strong CMEs (of Width > 105°) for 1997 – 2003

Figure 4 shows similar plots for very strong CMEs (of width > 105°). The top plots (a) are for SGN, as in Figure 1(a). The other plots (b) are for very strong CMEs. The following may be noted:

(1) All CME plots have two or more peaks (mostly two), none matching with the SGN peaks, which show latitudinal migration. Peaks in successive latitudes are not always simultaneous (*i.e.*, the joining lines are not always completely vertical), but systematic latitudinal migration is not indicated.
(2) No relationship with solar polar magnetic field reversals (full and hatched rectangles) is indicated.

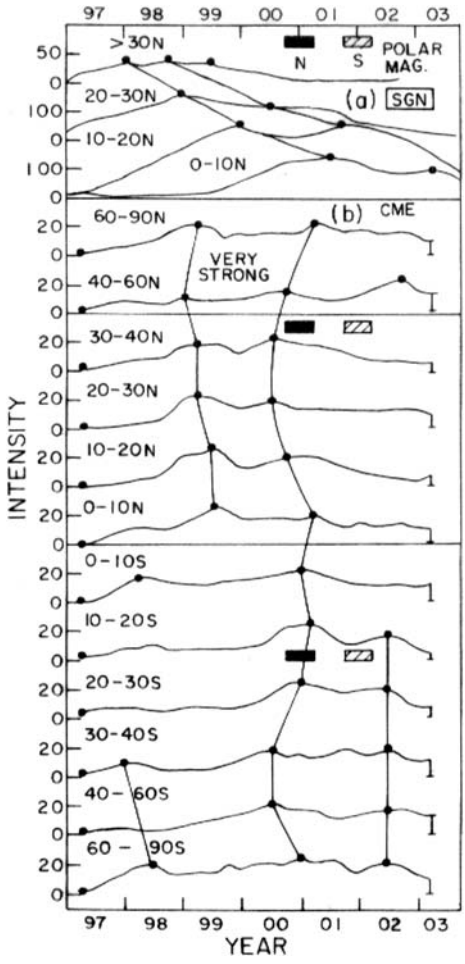

Figure 4 Same as Figure 1, but for very strong CMEs (of width > 105°)

(3) The numbers for 30° latitude belts are given in Table 1. There is a higher concentration in low latitudes, which drops to half at middle latitudes, and to less than one-third at polar latitudes.
(4) In contrast to Figure 1 where the initial value in 1997 was low, the CME values for 10° – 20° N, 0° – 10° N, and 0 – 10° S in Figure 3 (vertical bars) are very high, indicating that extra CME activity can occur in some low latitudes even at the beginning of sunspot activity.
(5) The Gnevyshev peaks and troughs in Figure 4 are almost similar to those in Figures 1, 2, and 3. Thus, the stronger CMEs do not have any special clarity of such peaks, in contrast to what was seen for some solar electromagnetic radiations, where the peaks were clearer for more energetic and intense events (X-ray flux, big sunspots, big flares, etc.; Feminella and Storini, 1997; Kane, 2002, 2003).

In summary, the evolutions of SGN and CMEs are very different from each other. The SGNs show latitudinal migration as in the butterfly diagram discovered by Maunder in 1904, also known as *Spörer's law*, whereas CME peaks remained steady. The dissimilarity is obvious visually, but a correlation analysis was carried out to get statistical evidence. For plots in

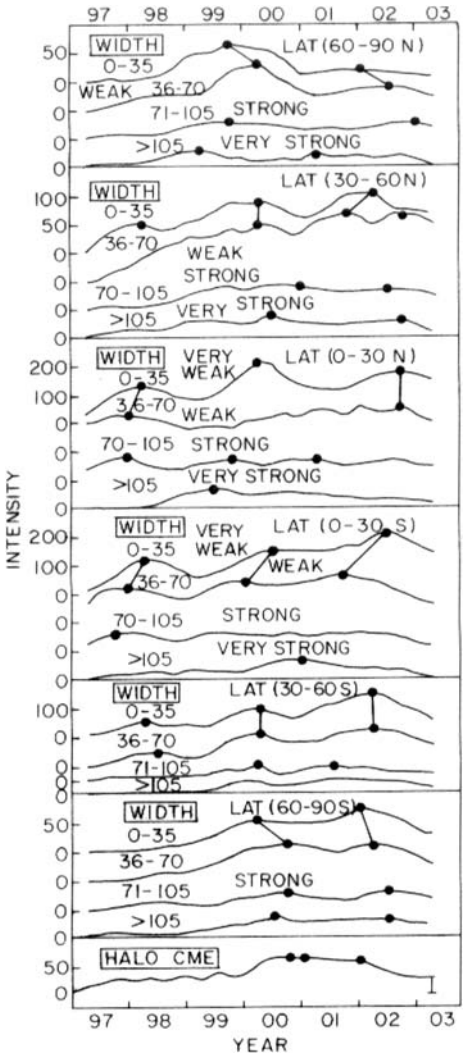

Figure 5 Plots of intensity and number of events of 12-month running means (four values per year) for 1997 – 2003, in six successive frames corresponding to six latitude belts (60° – 90° N, 30° – 60° N, 0° – 30° N, 0° – 30° S, 30° – 60° S, and 60° – 90° S). In each frame, there are four successive plots corresponding to CME widths of 0° – 35°, 36° – 70°, 71° – 105°, and > 105°. The maxima are indicated by big dots. Almost simultaneous maxima at successive latitudes for very weak and weak CMEs are joined by lines. The bottom plot is for halo CMEs (full disk, 360°).

Figure 1, the correlations between SGN and CMEs were +0.54 (0° – 10° N), +0.63 (10° – 20° N), +0.32 (20° – 30° N), and −0.28 (30° – 40° N), all of which are poor or moderate. Even for the best correlation of +0.63, the variance (square of correlation) explained is only ∼ 40%. In contrast, the correlations between the CMEs at different northern latitudes were very good between themselves (> + 0.90) for latitudes 0° – 40° N, slightly less so (+0.75) with 40° – 60° N, and moderate (+0.45) with 60° – 90° N. In the southern hemisphere, correlations were slightly less.

7. Direct Comparison of Plots for CMEs of Different Widths

To see how the variations of CMEs of different strengths (widths) compare with each other, Figure 5 shows the CME plots in six successive frames corresponding to six latitude belts

(60° – 90° N, 30° – 60° N, 0° – 30° N, 0° – 30° S, 30° – 60° S, and 60° – 90° S); in each frame, there are four successive plots corresponding to CME widths of 0° – 35°, 36° – 70°, 71° – 105°, and > 105°. The following may be noted:

(1) The Gnevyshev peaks (two or three) are more prominent in very weak and weak CMEs, as in the first two plots in each frame, and rather obscure in strong and very strong CMEs, as in the last two plots in each frame.
(2) The peaks in the very weak CMEs (first plot) do not match well with the peaks in weak CMEs (second plot).

Thus, with this mismatching and the mismatching of CME peaks with the peaks of SGNs mentioned earlier, it looks like the Gnevyshev peaks in CMEs occur independently, with no clear relation with other parameters, including solar polar magnetic field reversals.

In the very strong CME group (of width > 105°), there is an important subset, namely the *halo CMEs*, which are well related to geomagnetic disturbances. The halo CMEs cover the whole solar disk (360°). Their numbers were counted for successive three-month intervals and the 12-month running means were calculated. These are shown as the bottom plot of Figure 5. There are no prominent Gnevyshev peaks, only a broad plateau during 2000 – 2002. However, defining latitudes for very strong CMEs (*i.e.*, those with widths > 105°) is not very meaningful as their projection effects are large; projection effects are even stronger for the halo events.

8. Projection Effects

A detailed description of projection effects can be found in the Appendix of Hundhausen (1993). The problem is as follows. The SOHO LASCO CME Catalog lists CMEs with their PA measured from solar North in degrees (counterclockwise), angular widths, and speeds. These are observed on the plane of the sky and hence are a projection of the real values on that plane and are, therefore, apparent. Skirgiello (2003) attempted to eliminate these projection effects by assuming that events move radially and that their longitudinal distribution is uniform. A disconcerting finding was that events observed at higher latitudes were only apparent projections of events that really originated at lower latitudes. Later, Song, Feng, and Hu (2007) used the same idea but designed a simpler and easier new method with the same function as in Skirgiello (2003). The methodology is statistical and cannot be used for ascertaining the latitudes and longitudes of individual events. However, Song, Feng, and Hu (2007) found that the real CME latitude distribution had the following characteristics: (1) High-latitude CMEs ($\theta > 60°$, where θ is the latitude) constituted only 3% of all CMEs and mainly occurred during the time when the polar magnetic fields reversed sign. (2) Four percent of all CMEs occurred in the range $\theta = 45° – 60°$. These midlatitude CMEs occurred primarily in 2000, near the middle of 2002, and in 2005, forming a prominent three-peak structure. (3) The latitudinal evolution of low-latitude CMEs did not follow the Spörer sunspot law, which suggests that many CMEs originated outside of active regions.

It is gratifying to note that the item (3), obtained by allowing for the projection effects, is the same as the main result of the present investigation, namely, that low-latitude CMEs do not show latitudinal migration, unlike the SGNs, which obey the Spörer sunspot law. However, a curious fact is that Song, Feng, and Hu (2007) find less than 7% of CMEs in high latitudes whereas we find ∼ 19% in latitudes of 60° – 90° and 32% in latitudes of 30° – 60°, North and South combined. Thus, many of our middle and high-latitude CMEs must be from low and middle latitudes. If so, why are the plots in Figures 1 and 2 so different

for high and low latitudes? We suspect that the methodology of Song, Feng, and Hu (2007) underestimates the number of CMEs in high latitudes. This needs further exploration.

Regarding item (1), there is disagreement. Song, Feng, and Hu (2007) mention that high-latitude CMEs mainly occurred during the time when the polar magnetic fields reversed sign. This is a crude observation. Our results in Figures 1 and 2 show that, on a finer time scale, CME peaks occurred *several months earlier* (early 2000) than the beginning of the North Pole field reversal, which occurred in late 2000 to early 2001. Also, in lower latitudes, we see the first CME peak in 1998 – 1999, much earlier than the North Pole reversal. Gopalswamy *et al.* (2003, Figure 3) show a plot of monthly CME rates at high latitudes, show a CME fluctuation between the vertical lines marking the polar field reversals, and conclude that the field reversal is the cause of CME rate depressions. However, their figure also shows a big peak followed by a gap in the middle of 1999, much earlier than the north field reversal. The authors have mentioned this but give no explanation. We feel that the association of CME gaps with magnetic field reversals is, at best, tenuous.

9. Discussion and Conclusions

The sunspot number series at the peak of sunspot activity often has two or three peaks (Gnevyshev peaks; Gnevyshev, 1967, 1977). The sunspot group number data were examined for 1997 – 2003 (part of cycle 23) and compared with data for coronal mass ejection events for different widths, designated as very weak (of width $0° - 35°$), weak (of width $36° - 70°$), strong (of width $71° - 105°$), and very strong (of width $> 105°$), separately for the latitude belts $0° - 10°$, $10° - 20°$, $20° - 30°$, $30° - 40°$, $40° - 60°$, and $60° - 90°$ in northern and southern hemispheres of the Sun. The following may be noted:

(1) In SGN, there were mostly two Gnevyshev peaks in each of the four latitude belts ($0° - 10°$, $10° - 20°$, $20° - 30°$, and $> 30°$) in both northern and southern solar hemispheres. This pattern is different from what Gnevyshev (1967, 1977) reported for cycles 19 and 20. The SGNs were confined mostly to within $\pm 35°$ latitudes. These seemed to occur later in lower latitudes, indicating possible latitudinal migration as in Maunder butterfly diagrams (*i.e.*, Spörer sunspot law).
(2) In CMEs, very weak and weak CMEs showed prominent peaks during sunspot maximum years, and also during the declining phase. The CME activity lasted longer than the SGN activity. However, the *CME peaks did not match with the* SGN *peaks* and were almost simultaneous at different latitudes, indicating no latitudinal migration. In strong and very strong CMEs (including halo CMEs), the Gnevyshev peaks were obscure and ill-defined.
(3) The solar polar magnetic fields show polarity reversal during sunspot maximum years, first at the North Pole and, a few months later, at the South Pole. *The CME peaks and gaps did not match with the magnetic field reversal times and occurred several months earlier.* Thus, the explanation that Gnevyshev gaps are caused by solar polar magnetic field reversals does not seem to be true. Effects cannot precede the cause.
(4) The correlations between SGN and CMEs was ~ 0.60 or less in low latitudes, implying an explained variance of $\sim 40\%$.

The first peak – gap sequence in SGN as well as CME frequency started in 1998 – 1999, long before the North Pole magnetic field reversal in late 2000 to early 2001. The second peak – gap sequence in CME also started several months earlier than the North Pole field reversal. As such, the field reversals cannot be the cause of the CME and sunspot gap GGs.

We feel that, whereas solar activity does not rise smoothly and fall smoothly with a single peak, the multiple peak structure during the solar activity maximum reflects solar dynamical upheavals and turmoil and perhaps magnetic field structure reorganizations, which manifest in different parameters (*e.g.*, sunspots, CMEs, and polar field reversals) with different phases, and none of these parameters seem to be the cause of the fluctuations in the other parameters. The turmoil seems to occur at all latitudes, in low and middle latitudes where sunspots are confined, and at high latitudes where field reversals occur, but independently of each other, probably because different physical mechanisms are involved for different parameters.

Acknowledgements The CME catalog is generated and maintained at the CDAW Data Center by NASA and The Catholic University of America in cooperation with the Naval Research Laboratory. SOHO is a project of international cooperation between ESA and NASA. Thanks are owed to the referee for valuable suggestions. This work was partially supported by Fundação Nacional de Desenvolvimento Científico e Tecnológico (FNDCT), Brazil, under Contract No. FINEP-537/CT.

References

Alania, M.V., Baranov, D.G., Tyasto, M.I., Vernova, E.S.: 1999, *Proc. 26th ICRC* **7**, 131.
Antalova, H., Gnevyshev, M.N.: 1965, *Astron. Z.* **42**, 253.
Antalova, H., Gnevyshev, M.N.: 1983, *Contrib. Astron. Obs. Skaln. Pleso* **11**, 63.
Bilenko, I.A.: 2002, *Astron. Astrophys.* **396**, 657.
Cliver, E.W., Hudson, H.S.: 2002, *J. Atmos. Solar-Terr. Phys.* **64**, 231.
Durant, C.J., Wilson, P.R.: 2003, *Solar Phys.* **214**, 23.
Feminella, F., Storini, M.: 1997, *Astron. Astrophys.* **322**, 311.
Gnevyshev, M.N.: 1967, *Solar Phys.* **1**, 107.
Gnevyshev, M.N.: 1977, *Solar Phys.* **51**, 175.
Gopalswamy, N., Lara, A., Yashiro, S., Nunes, S., Howard, R.A.: 2003, *Astrophys. J.* **598**, L63.
Harvey, K.L., Recely, F.: 2002, *Solar Phys.* **211**, 31.
Hundhausen, A.J.: 1993, *J. Geophys. Res.* **98**, 13177.
Jokipii, J.R., Thomas, B.: 1981, *Astrophys. J.* **243**, 1115.
Kane, R.P.: 2002, *Ann. Geophys.* **20**, 741.
Kane, R.P.: 2003, *J. Geophys. Res.* **108**(A1), 1046. doi:10.1029/2002JA009542.
Kane, R.P.: 2006a, *Solar Phys.* **233**, 107.
Kane, R.P.: 2006b, *Solar Phys.* **236**, 207.
Kane, R.P.: 2008, *Solar Phys.* in press.
Munro, R.H., Gosling, J.T., Hildner, E., MacQueen, R.M., Poland, A.I., Ross, C.L.: 1979, *Solar Phys.* **61**, 201.
Obridko, V.N., Shelting, B.D.: 1992, *Solar Phys.* **137**, 167.
Skirgiello, M.: 2003, *Geophys. Res. Lett.* **30**, 1995. doi:10.1029/2003GL017618.
Song, W., Feng, X., Hu, Y.: 2007, *Astrophys. J.* **667**, L101.
Storini, M., Pase, S.: 1995, In: Watanabe, T. (ed.) *Proc. 2nd SOLTIP Symp., STEP GBRSC News* **5**, 255.
Storini, M., Bazilevskaya, G.A., Fliickiger, E.O., Krainev, M.B., Makhmutov, V.S., Sladkova, A.I.: 2003, *Adv. Space Res.* **31**(4), 895.
Tousey, R.: 1973, In: Rycroft, M.J., Runcom, S.K. (eds.) *The Solar Corona*, Springer, New York, 173.
Webb, D.F., Howard, R.A.: 1994, *J. Geophys. Res.* **99**, 4201.